Aging End product in Iris Biometrics

Dr.Kashif Qureshi

Department Of Computer Science, tel: +966 (0)535598451,Jazan University, Jazan, Saudia
srk1521@gmail.com

Abstract

It has been widely accepted that iris biometric systems are not subject to a template aging effect. Recently presented the first published evidence of a template aging effect, using images acquired from 2004 through 2008 with an LG 2200 iris imaging system, representing a total of 13 subjects (26 irises). We report on a template aging study involving two different iris recognition algorithms, a larger number of subjects (43), a more modern imaging system (LG 4000), and over a shorter time-lapse (2 years). We also investigate the degree to which the template aging effect may be related to pupil dilation and/or contact lenses. We find evidence of a template aging effect, resulting in an increase in match hamming distance and false reject rate.

1. Introduction

The assumption that the appearance of the iris is stable throughout a person's lifetime has been accepted by the research community since the beginnings of iris biometric research. Daugman's statement, "As an internal (yet externally visible) organ of the eye, the iris is well protected and stable over time" has been echoed in similar form in many publications [5-9].

It is important to make a distinction between the terms "template aging effect" and "iris aging effect." A template aging effect occurs when the quality of the match between an enrolled biometric sample and a sample to be verified degrades with increased elapsed time between the two samples. In our experiment, we test for the presence of a template aging effect over an approximately two-year time lapse, and find that one does exist. An "iris aging effect," on the other hand, would be some definite change in the iris texture pattern due to human aging. An iris aging effect would generally imply a template aging effect in the field of iris biometrics. However, observing a template aging effect would not necessarily imply that an iris aging effect exists. For example, if the average pupil dilation changes over time, this might affect the observed iris texture in a way that causes, at least partially, a template aging effect. We explore the possibility of a template aging effect both including and independent of dilation as well as several other factors.

1.1. Related work

At present evidence of a significant effect of time-lapse between images on iris recognition. Their experiments used images taken by an LG 2200 camera from data acquisitions in 2004 through 2008, acquired approximately weekly throughout the semester. The dataset used in their experiments contains images from only 13 different subjects, or only 26 irises. They use statistical tests on the means of their Hamming distance distributions to make their analyses, but do not present false reject rates over a range of feasible decision thresholds. The LG 2200, which at the time of their data acquisition may have been considered a state-of-the-art system, is no longer marketed. Also, because of the technology used in the system, as Bowyer and Flynn document, there is a possibility of interlace artifacts in the images taken if there is significant subject motion during image acquisition.

Our experiments improve on these aspects of the report by Baker *et al.* [1]. We test our data on two different segmentation and matching algorithms. We use an LG 4000 system which is currently state-of-the-art and is based on more modern technology than the LG 2200. Our dataset contains over three times the number of subjects as that of . We present the false reject rates at a fractional Hamming Distance decision threshold ranging from 0.28 to 0.34 and Verify eye match scores between 30 and 120. We also use statistical tests analogous to their methods and compare images with approximately two years time-lapse rather than four.

Finally, we treat other possible factors for degradation of match quality in a different manner than Baker *et al.*. In their work, they reported no correlation between the mean change in hamming distance from short to long time-lapse and the mean change in dilation difference of

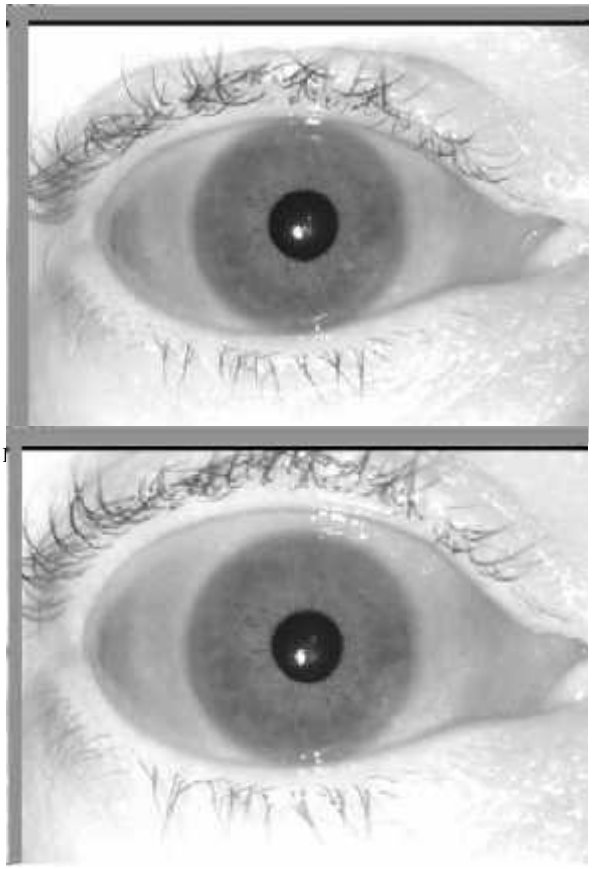

Figure 2: Subject 02463 verification image from 2008. The short time-lapse comparison with the image in Figure 1 resulted in a

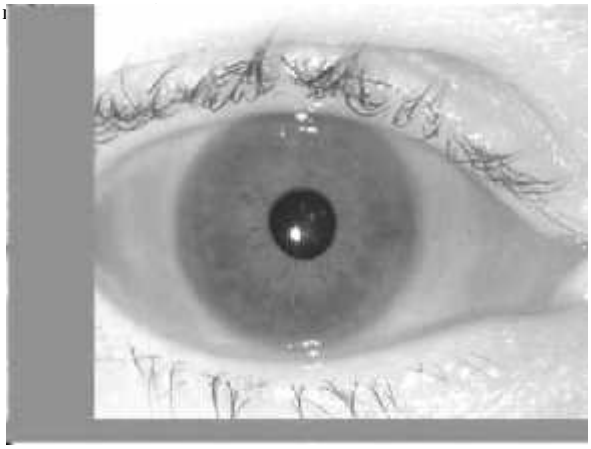

Figure 3: Subject 02463 verification image from 2010. The long time-lapse comparison with the image in Figure 1 resulted in a normalized HD of 0.0447158 and a Verify Eye match score of 775.

match comparisons from short to long time lapse. Instead of looking at correlation between dilation difference and hamming distance, we screen for dilation difference by analyzing a subset of images with small dilation difference. Baker *et al.* also cite the effects of contact lenses on the match distribution, but simply report the number of subjects with or without contacts. We analyze a subset of images containing only those subjects who did not wear contacts in any session.

2. Experimental Stuff

The images used in this experiment were all acquired using the same LG 4000, in the same laboratory, following the same image acquisition procedure. Images from 43 participants, or 86 irises, were used. Of these subjects, 22 were male and 21 were female, and 39 were Caucasian, 2 were Asian, 1 was Hispanic, and 1 did not provide information on ethnicity. The ages of subjects ranged from 21 to 63 years as of 2010, with an average of 31. Images were taken approximately weekly during 6 sessions in the spring semester of 2008 and approximately biweekly during 4 sessions in the spring semester of 2010. Of 1830 total images, 1042 were acquired in 2008 and 788 in 2010.

We use two different iris recognition systems. The first is our own implementation of software based on IrisBEE , using a Canny edge detector, Hough transform, and 1-D log-Gabor filters to segment and then analyze the texture of the iris. The software also contains improvements described . The second software implementation is the VeriEye SDK, developed by Neurotechnology.

The calculation of the accuracy of a comparison of two iris images differs between the two algorithms. Iris BEE generates fractional Hamming distances (HDs), which range from 0 to 1, with 0 being a perfect match. Verify Eye generates a match score ranging from 0 to 3235, with 3235 being a perfect match and 0 being a no match comparison.

3. Experimental Method

We define a long time-lapse comparison as a comparison between one image from 2008 and one from 2010. A short time-lapse comparison is a comparison between two images from the same year. Images of the same iris taken on the same day are not compared against each other. The dates of acquisition are such that the short time-lapse comparisons range from 5 to 51 days apart, and the long time-lapse comparisons range from 665 to 737 days apart.

3.1. Analysis of false reject rates

The image dataset is analyzed to generate match and non-match distributions for both the short time-lapse case and the long time-lapse case. For each subset described below, there are N_1 comparisons in the match distribution for the short time-lapse case and N_2 comparisons in the match distribution for the long time- lapse case. There are N_3 comparisons in the non-match distribution for the short time-lapse case and N_4 comparisons in the non-match distribution for the long time-lapse case. These four values can be found in Table 1. We calculate the false reject rates for the two different match distributions over a range of possible decision threshold values. These false reject rates are tabulated to show their difference between the short time-lapse case and the long time-lapse case.

3.2. Screening on difference in pupil dilation

The degree of dilation of an eye affects the distribution of match scores. A comparison of two images of high dilation ratios produces a higher HD than a comparison of two images of small dilation ratios. A comparison of two images of large delta, or difference in dilation, will have a higher HD than that of small delta. We create a subset of the original set of data, eliminating comparisons with a delta greater than 0.1. In the small delta subset, three iris subjects were eliminated due to a lack of long time-lapse comparisons within the subject, leaving this subset with 83, rather than iris subjects.

While it may be possible to control for dilation during enrollment, it is likely impractical to attempt to control this during verification. Analyzing a subset of matches that correspond to only those with small difference in dilation does not correspond to actual operation of any iris biometric system that we are aware of. Nor are we proposing that this is a practical restriction to enforce for typical applications. Our goal is simply to investigate the degree to which a change in the difference in pupil dilation may be involved in the template aging effect.

3.3. Screening on presence of contact lenses

Contact lenses have been shown to degrade match quality . In our dataset, 29 subjects did not wear contacts in any session. Nine wore contacts in all participating sessions for both years, two of which changed contact type between years. Five subjects wore contacts in some sessions but not others. We also analyze subsets of the previously mentioned datasets with only those subjects who did not wear contacts in any session. We note in this case also that it would be difficult in a real-world implementation of an iris recognition system to control for the presence of contact lenses.

	Short Matches	Long Matches	Short Non-matches	Long Non-matches
Original	8631	9837	673640	811259
Small Delta	8443	7769	418573	485019
No Contacts	6432	7326	337225	400131
No Contacts, Small Delta	6292	5722	202854	226653

3.4. Adjustment for number of iris code bits used

In order to account for the number of bits used in comparisons of two iris codes, we implement Daugman's square root score normalization technique across all sets of data. Some very low raw hamming distances can become negative after normalization, as shown in Figures 4 and 6. The scaling parameter for this dataset, the average number of bits used per comparison, was 904. Note that this adjustment only applies for the Iris BEE data, and not the Verify Eye data.

3.5. Statistical tests on the means

The tabulation of false reject rates across a range of feasible decision thresholds is a more practically useful result, but it is important to consider how this is related to results of statistical tests such as those of Baker *et al.* . These tests follow the experimental method used by Baker *et al.*. The tests are performed using the same methodology for both Iris BEE and Verify Eye data, but so as not to be redundant, we will describe our methods only in terms of Hamming Distance and not the Verify Eye match score. We consider the null hypothesis that the fractional Hamming Distance (HD) for matches between long time-lapse images is not greater than that for matches between short time-lapse images, and the alternative that the HD for long time-lapse comparisons is greater than that of short time-lapse comparisons. We take the average match HDs for each subject from the short time-lapse and subtract them from those of the long time-lapse. We perform a sign test on these differences with the null hypothesis that a positive difference occurs as often as a negative difference, and the alternative that a positive difference occurs more often than a negative. When the data is found to be approximately normal using a chi-square goodness-of-fit test, we also perform a t-test on the differences of means with the null hypothesis that the differences come from a distribution with mean zero, and the alternative that the distribution has a mean greater than zero.

4. Results

4.1. Original dataset

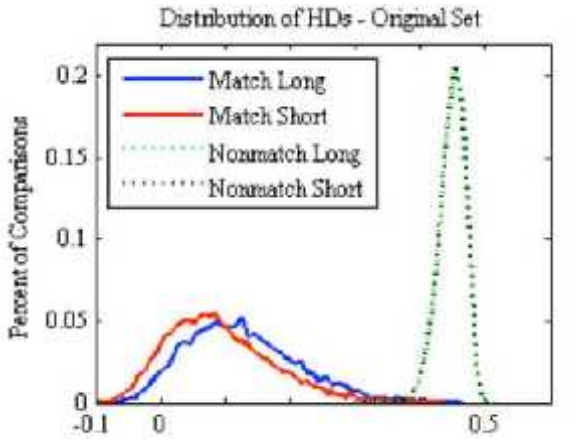

Figure 4: The match distribution for the long time-lapse is clearly shifted right on the short lapse distribution, while the non-match distributions have no apparent difference.

4.1.1. Iris BEE The match and non-match distributions for our original short time-lapse and long time-lapse datasets are plotted in Figure 4. There is no discernible difference in the non-match distributions. However, there clearly is a difference in the match distributions. The false reject rates for the two distributions, computed for a range of decision thresholds from 0.28 to 0.34, are in Table 2. The FRR for the short time-lapse distribution varies from 1.9% at a threshold of 0.28 to 0.4% at 0.34. In comparison, the FRR for the long time-lapse distribution varies from 4.9% at 0.28 to 1.5% at 0.34. The increase in FRR from short to long time-lapse ranges from approximately 157% at 0.28 to 305% at 0.34. This increase is relatively stable between thresholds of 0.30 to 0.32, varying between 215% and 210%. From these results, it is clear that there is a sizeable increase in false reject rate between the short and long time-lapse distributions over the entire range of feasible decision threshold values. Thus, Figure 4 shows clear evidence of a template aging effect for iris biometrics.

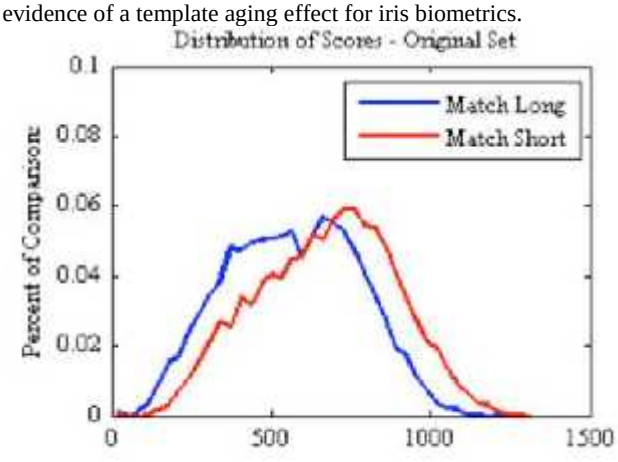

Figure 5: The match distribution for long time-lapse is clearly shifted to the left of the short time-lapse distribution. For Verify Eye, higher scores indicate a better match between images.

Table 2: False reject rates of all sets of images for both short and long time-lapse, using the Iris BEE algorithm.

Threshold HD	Original Short	Original Long	% Increase	No Contacts Short	No Contacts Long	% Increase
0.28	0.0192	0.0493	156.8	0.0230	0.0601	161.3
0.29	0.0152	0.0393	158.6	0.0176	0.0475	170.0
0.30	0.0102	0.0321	214.7	0.0115	0.0386	235.7
0.31	0.0081	0.0255	214.8	0.0090	0.0300	233.3
0.32	0.0068	0.0211	210.3	0.0073	0.0246	236.7
0.33	0.0053	0.0179	237.7	0.0053	0.0202	281.1
0.34	0.0038	0.0154	305.3	0.0036	0.0168	466.7
Threshold HD	Small Delta Short	Small Delta Long	% Increase	No Contacts Small Delta Short	No Contacts Small Delta Long	% Increase
0.28	0.0167	0.0366	119.2	0.0205	0.0433	111.2
0.29	0.0131	0.0295	125.2	0.0157	0.0343	118.5
0.30	0.0086	0.0245	184.9	0.0103	0.0278	169.9
0.31	0.0069	0.0198	187.0	0.0083	0.0218	162.7
0.32	0.0060	0.0167	178.3	0.0072	0.0182	152.8
0.33	0.0046	0.0143	210.9	0.0052	0.0149	186.5
0.34	0.0031	0.0130	319.4	0.0035	0.0131	274.3

Table 3: False reject rates of all sets of images for both short and long time lapse, using the VeriEye algorithm.

Threshold Score	Original Short	Original Long	% Increase	No Contacts Short	No Contacts Long	% Increase
30	2.32E-04	9.17E-04	194.7	0	0	nan
40	2.32E-04	0.0010	238.6	0	1.37E-04	inf
50	2.32E-04	0.0010	238.6	0	1.37E-04	inf
60	2.32E-04	0.0010	238.6	0	1.37E-04	inf
70	2.32E-04	0.0011	282.4	0	2.73E-04	inf
80	2.32E-04	0.0011	282.4	0	2.73E-04	inf
90	2.32E-04	0.0015	457.9	0	8.20E-04	inf
100	3.48E-04	0.0022	443.3	1.56E-04	0.0018	940.6
110	5.81E-04	0.0029	291.2	4.67E-04	0.0025	326.4
120	6.97E-04	0.0040	370.2	6.23E-04	0.0038	414.2
Threshold Score	Small Delta Short	Small Delta Long	% Increase	No Contacts Small Delta Short	No Contacts Small Delta Long	% Increase
30	2.37E-04	0.0012	289.1	0	0	nan
40	2.37E-04	0.0013	343.5	0	1.75E-04	inf
50	2.37E-04	0.0013	343.5	0	1.75E-04	inf
60	2.37E-04	0.0013	343.5	0	1.75E-04	inf
70	2.37E-04	0.0013	343.5	0	1.75E-04	inf
80	2.37E-04	0.0013	343.5	0	1.75E-04	inf
90	2.37E-04	0.0017	506.5	0	7.00E-04	inf
100	3.56E-04	0.0025	488.4	1.59E-04	0.0018	899.3
110	5.93E-04	0.0031	321.7	4.78E-04	0.0025	313.0
120	7.12E-04	0.0037	325.4	6.37E-04	0.0032	294.7

4.1.2. Verify Eye The match distributions for the original short and long time-lapse datasets are plotted in Figure 5. The non-match distributions are not plotted because over 80% of the data have scores of ₀, and do not show on the graph. A clear shift in the match distributions is visible. The false reject rates for the two distributions over a match score threshold ranging from 30 to 120 are compiled in Table 3. The FRR for short time-lapse varies from 0.02% at a threshold of 30 to 0.07% at 120. The FRR for long time-lapse varies from 0.09% at 30 to 0.4% at 120. The increase in FRR from short to long time-lapse ranges from 195% at a threshold of 30 to 370% at 120, with a maximum of 457% at 90. It is clear that there is a significant increase in false reject rate between short and long time-lapse distributions over the range of feasible threshold values.

4.2. Dataset screened on pupil dilation

4.2.1. Iris BEE The false reject rates for the short time- lapse distribution ranged from approximately 1.7% at a decision threshold of 0.28 to 0.3% at 0.34. Comparatively, the long time-lapse FRRs ranged from 3.7% to 1.3% across that span. The increase in FRR from short to long time-lapse varies from 119% at 0.28 to 319% at 0.34. Like the original set in section 4.1, the increase in FRR for the set experienced relative stability between thresholds of 0.30 and 0.32, varying between 178% and 187%. The plots of the match and non-match distributions for both short and long time-lapse can be found in Figure 6.

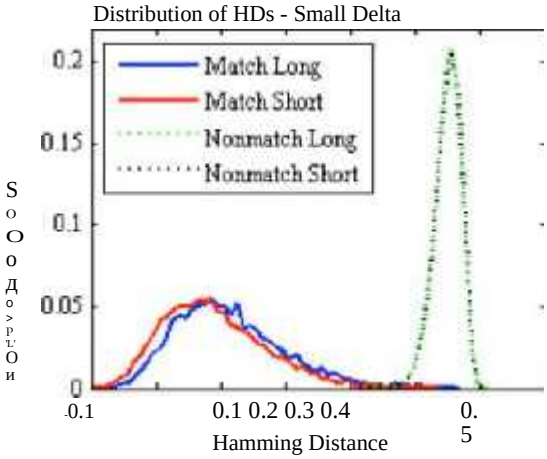

Figure 6: Again, the non-match distributions lie on top of each other while the match distributions are clearly separated.

4.2.2. Verify Eye The false reject rates for short time-lapse ranged from approximately 0.02% at a threshold of 30 to 0.07% at 120. In comparison, the long time-lapse FRRs ranged from 0.1% at 30 to 0.4% at 120. The increase in FRR from short to long time-lapse varied from 289% at 30 to 325% at 120, with a maximum of 507% at a threshold of 90. The plots of the match distributions for short and long time-lapse are displayed in Figure 7.

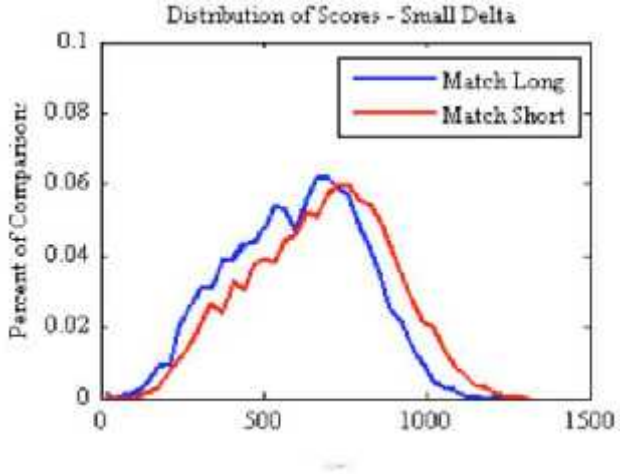

Verify Eye Match Score Figure 7: The long time-lapse distribution for the small delta dataset is shifted significantly to the left of the short time-lapse distribution.

4.3. Dataset screened on contact lenses

4.3.1. Iris BEE The false reject rates for the short time-lapse case for this dataset ranged from 2.3% at a threshold of 0.28 to 0.4% at a threshold of 0.34. The long time-lapse false reject rates ranged from $_{6.0}$% to 1.7%. The increase in FRR from short to long time-lapse varies from 161% at 0.28 to 467% at 0.34. Similar increases in false reject are observed between thresholds of 0.30 and 0.32, varying between 233% and 237%. The match distribution plots for this and future cases, for both IrisBEE and VeriEye, are similar to the previous datasets, and are not included due to space limits.

4.3.2. VeriEye The false reject rates for the short time-lapse ranged from $_{0.02}$% at a threshold of $_{100}$ to 0.06% at 120. No match comparisons had a score of 90 or below. The long time-lapse FRRs ranged from 0.01% at 40 to 0.4% at 120, with no match comparisons yielding a score of 30 or below. The

4.3.3. measurable increases in FRR for thresholds of 100, 110 and 120 were 941%, 326%, and 414%, respectively.

4.4. Dataset screened on dilation and contacts

4.4.1. Iris BEE The false reject rates for the final dataset ranged from 2.1% at a decision threshold of 0.28 to 0.4% at a threshold of 0.34 in the short time-lapse case. The long time-lapse FRRs varied between 4.3% at 0.28 to 1.3% at 0.34. The observed increase in FRR differs between 111% and 274%. Between thresholds of 0.30 and 0.32, where relative stability has been noted in previous sections, the FRRs ranged from 153% to 170%.

4.4.2. Verify Eye The false reject rates for the short time-lapse case ranged from $_{0.02}$% at a threshold of $_{100}$ to 0.07% at 120. No match comparisons had a score of 90 or below. The FRRs for long time-lapse ranged from 0.02% at 40 to 0.3% at 120, with no match comparisons yielding a score of 30 or lower. The measurable increases in FRR for thresholds of 100, 110, and 120 were 899%, 313%, and 295%, respectively.

4.5. Statistical tests on the means

The results of the statistical tests described in Section 3.6 are as follows. For Iris BEE, all four datasets rejected the null hypothesis of the sign test. Of the two whose distributions of mean HDs were found to be approximately normal, both also rejected the null hypothesis of the t-test. The p-values of those statistical tests, as well as the overall mean HDs of the distributions, can be found in Table 4. Similar results were found for the tests using VeriEye. In the sign test, all four datasets rejected the null hypothesis. None of the distributions were found to be normal, so t-tests were not performed. These results can be found in Table 5.

Table 4: Results of statistical tests for each dataset, using Iris BEE.

	Match Comparison HD			Non-match Comparison HD			# Irises w/ Increased HD	p-values	
Dataset	Short	Long	Change	Short	Long	Change		Sign Test	T-Test
Original	0.0900	0.1250	0.0350	0.4481	0.4482	0.0001	84/86	9.67E-23	N/A
Small Delta	0.0884	0.1113	0.0229	0.4483	0.4483	0.0000	79/83	4.00E-19	N/A
No Contacts	0.0964	0.1317	0.0353	0.4483	0.4483	0.0000	56/58	1.19E-14	7.91E-14
No Cont., Sm. Del.	0.0950	0.1177	0.0227	0.4486	0.4485	-0.0001	52/55	1.54E-12	7.67E-11

Table 5: Results of statistical tests for each dataset, using VeriEye.

	Match Comparison HD			Non-match Comparison HD			# Irises w/ Deer. Score	p-values	
Dataset	Short	Long	Change	Short	Long	Change		Sign Test	T-Test
Original	670.4	566.3	-104.1	0.981	0.962	-0.019	82/86	5.76E-20	N/A
Small Delta	673.7	599.0	-74.7	0.943	0.926	-0.017	78/83	6.40E-18	N/A
No Contacts	620.3	519.1	-101.2	0.858	0.846	-0.012	54/58	3.17E-12	N/A
No Cont., Sm. Del.	623.7	551.0	-72.7	0.792	0.777	-0.015	52/55	1.54E-12	N/A

5. Summary and discussion

We report on the results of an experimental investigation of template aging in iris biometrics. Here, a "template aging effect" is defined as an increase in the false reject rate with increased elapsed time between the enrollment image and the verification image. We find that a template aging effect does exist. We also consider controlling for factors such as difference in pupil dilation between compared images and the presence of contact lenses, and how these affect template aging, and we use two different algorithms to test our data.

While our experimental results support those of Baker *et al*. [1] in concluding that a template aging effect does exist in iris biometrics, our work is distinguished from that of Baker *et al.* [1] in several respects. First, our iris image dataset represents a larger number of different subjects and irises (86 irises vs. 26), and is acquired using a more modern iris imaging system (LG 4000 vs. LG 2200). Second, we consider an elapsed time interval that is shorter than that considered by Baker *et al.* (~2 years vs. ~4 years). Thirdly, we take a different approach to handling potential confounding factors such as pupil dilation and contact lenses. We create data subsets with only those comparisons with a difference in dilation between images of 0.1 or less, whereas Baker *et al*. simply report that there is no linear correlation between dilation difference and hamming distance across time- lapse. We also create subsets with only those subjects who did not wear contact lenses in any session; Baker *et al.* only report the number of contact wearers. Finally, we use two different algorithms, Iris BEE and Verify Eye, to test our data.

Our primary experimental result involves an image dataset representing 86 different irises. For each iris, match and non-match distributions were created for a short time-lapse case (5 to 51 days elapsed) and a long time-lapse case (665 to 737 days elapsed). We observe no significant difference in the non-match distribution between the short time-lapse data and the long time- lapse data. However, we do observe a shift in the match distribution, such that there is an increase in false reject rate across the range of potential decision threshold values. Using a threshold fractional Hamming Distance of 0.32 for the experiments run using IrisBEE, the observed false reject rate increases by 210% from the short time-lapse match distribution to the long time-lapse match distribution. The increase in false reject rate ranges from 157% at a threshold of 0.28 to 305% at 0.34. Note that the false reject rate is in the area in the tail of the match distribution, so it naturally decreases as the decision threshold moves further toward the tail. Because the amount of data in the tail of the distribution also decreases with increased values of the decision threshold, we can expect that the estimated magnitude of increase in false reject rate between the two match distributions is more subject to noise. The experiments run using the VeriEye algorithm yielded similar results. The observed false reject rate increases from short to long time-lapse by 195% at a threshold of 30 and up to 457% at a threshold of 100. As described above, the tail of the distribution, in this case lower scores, is subject to noise due to limited data, however, it is clear from these results that a template aging effect is present.

Following this initial result, we investigated factors that could possibly contribute to the observed increase in false reject rate. One possible confounding factor is the difference in pupil dilation between two images in a comparison. We found that for IrisBEE, restricting the dataset to image comparisons that had only a small difference in pupil dilation resulted in a smaller increase overall in FRR. The results from VeriEye showed a slightly larger increase in FRR overall. Thus, depending on the algorithm, pupil dilation may or may not be a significant confounding factor for measuring a template aging effect. Another potential factor is the presence of contact lenses. We found that after using only those subjects who did not wear contacts in any session, the results of both algorithms showed a larger increase in false reject rate than the original dataset. However, this comparison involved a large decrease in the number of irises represented, and both the sets controlling for contacts and those controlling for dilation experienced a large decrease in the number of match comparisons, which may make these sets of results less reliable.

Based on the above results, we conjecture that iris biometric systems that are able to restrict comparisons to images with a small difference in dilation may be subject

to a somewhat smaller template aging effect. Also, screening for this factor as well as the presence of contact lenses is partially additive; that is, restriction to small dilation difference and the absence of contact lenses lead to slightly better performance across a longer time lapse than pupil dilation alone.

It is not possible from our current results to give a precise estimate of the magnitude of the template aging effect to expect in a practical application or a specific correlation between template aging and elapsed time for iris biometrics in general. The observed increase in false reject rate naturally varies with a number of factors. These include, likely among other important reasons, the decision threshold of the system, the inherent accuracy of the segmentation algorithms, the variation in pupil dilation, and the presence of contact lenses. A better estimate of the magnitude of the general template aging effect and of all its underlying causes requires additional research using larger datasets.

The existence of a template aging effect should not prevent iris biometrics from practical use. Much like other identification methods such as drivers' licenses are renewed after a set period of time, a subject could be reenrolled into the system, once an acceptable time frame is determined. Further research on the changes in iris texture over time will also increase our understanding of both the nature and location of such changes. In some sense, these findings place iris biometrics on equal ground with other biometric areas in which the existence of a template aging effect has already been acknowledged. We know of no studies that present any conclusion about the relative speed of template aging in different biometrics.

References

[1] S. Baker, K. W. Bowyer, and P. J. Flynn, "Empirical evidence for correct iris match score degradation with increased time-lapse between gallery and probe matches," in *Proc. Int. Conf. on Biometrics*, pp. 1170-1179, 2009.

[2] J. Daugman, "How Iris Recognition Works," *IEEE Trans. Circuits and Sys. For Video Tech*, vol. 14, pp. 21-30, Jan. 2004.

[3] http://www.irisid.com/ps/products/previousmodels/ irisaccess2200.htm. Accessed July 2010.

[4] http://www.irisid.com/ps/products/irisaccess4000.htm, Accessed July 2010.

[5] J. Thornton, M. Savvides, V. Kumar. "A Bayesian Approach to Deformed Pattern Matching of Iris Images," *IEEE Trans. PAMI.*, vol. 29, pp. 596- 606, Apr. 2007.

[6] D. Monro, S. Rakshit, D. Zhang. "DCT-Based Iris Recognition," *IEEE Trans. PAMI.*, vol. 29, pp. 586-595, Apr. 2007.

[7] K. Miyazawa, K. Ito, T. Aoki, K. Kobayashi, H. Nakajima. "An Effective Approach for Iris Recognition Using Phase-Based Image Matching," *IEEE Trans. PAMI*, vol. 30, pp. 1741-1756, Oct. 2008.

[8] A. Ross, "Iris Recognition: The Path Forward," *Computer*, vol. 43, no. 2, pp. 30-35, Feb. 2010.

[9] M. S. Hosseini, B. N. Araabi, H. Soltanian-Zadeh, "Pigment Melanin: Pattern for Iris Recognition," *IEEE Trans. Instrumentation and Measurement*, vol. 59, pp. 792-804, April 2010.

[10] N. Kalka, J. Zui, N. Schmid, B. Cukic, "Image Quality Assessment for Iris Biometric", *SPIE 6202: Biometric Technology for Human Identification III*, Orlando, FL, 2006.

[11] K. P. Hollingsworth, K. W. Bowyer, and P. J. Flynn, "Pupil dilation degrades iris biometric performance," *Computer Vision and Image Understanding*, vol. 113, no. 1, pp. 150-157, Jan. 2009.

[12] S. Ring and K. Bowyer, "Detection of Iris Texture Distortions by Analyzing Iris Code Matching Results," in *2008 IEEE Conf. on Biometrics: Theory, Applications, and Systems*, Arlington, VA, 2008.

[13] J. Daugman, "New Methods in Iris Recognition," *IEEE Trans. Sys., Man, and Cyber*. vol. 37, pp. 1167-1175, Oct. 2007.

[14] K. W. Bowyer and P. J. Flynn. "The ND-IRIS-0405 iris image dataset," Technical report, Univ. of Notre Dame, Notre Dame, IN, 2009, http://www.nd.edu/~cvrl/papers/ND-IRIS-0405.pdf.

[15] P. Grother, E. Tabassi, G. W. Quinn, and W. Salamon. "Performance of Iris Recognition Algorithms on Standard Images," Technical report, National Institute of Standards and Technology, September 2009. Published as NIST Interagency Report 7629, http://iris.nist.gov/irex/irex_summary.pdf.

[16] National Institute of Standards and Technology. Iris Challenge Evaluation, 2006, http://iris.nist.gov/ice.

[17] X. Liu, K. Bowyer, P. Flynn. "Experiments with an improved iris segmentation algorithm," Fourth IEEE Workshop on Automatic Identification Technologies, 118123, Oct 2005.

[18] Xiaomei Liu. "Optimizations in Iris Recognition." PhD Dissertation, University of Notre Dame, 2006.

[19] http://www.neurotechnology.com/. Accessed Oct. 2010.

[20] www.wikipedia.com